

(Faster) Multi-Sided Boundary Labelling*

Prosenjit Bose¹, Saeed Mehrabi¹, and Debajyoti Mondal²

¹School of Computer Science, Carleton University, Ottawa, Canada.

`jit@scs.carleton.ca`, `saeed.mehrabi@carleton.ca`

¹Department of Computer Science, University of Saskatchewan, Saskatoon, Canada.

`d.mondal@usask.ca`

Abstract

A *1-bend boundary labelling* problem consists of an axis-aligned rectangle B , n points (called *sites*) in the interior, and n points (called *ports*) on the labels along the boundary of B . The goal is to find a set of n axis-aligned curves (called *leaders*), each having at most one bend and connecting one site to one port, such that the leaders are pairwise disjoint. A 1-bend boundary labelling problem is k -sided ($1 \leq k \leq 4$) if the ports appear on k different sides of B . Kindermann et al. [“Multi-Sided Boundary Labeling”, *Algorithmica*, 76(1): 225-258, 2016] showed that the 1-bend three-sided and four-sided boundary labelling problems can be solved in $O(n^4)$ and $O(n^9)$ time, respectively. Bose et al. [SWAT, 12:1-12:14, 2018] improved the latter running time to $O(n^6)$ by reducing the problem to computing maximum independent set in an outerstring graph. In this paper, we improve both previous results by giving new algorithms with running times $O(n^3 \log n)$ and $O(n^5)$ to solve the 1-bend three-sided and four-sided boundary labelling problems, respectively.

1 Introduction

Map labelling is a well-known problem in cartography with applications in educational diagrams, system manuals and scientific visualization. Traditional map labelling that places the labels on the map such that each label is incident to its corresponding feature, creates overlap between labels if the features are densely located on the map. This motivated the use of *leaders* [15, 9]: line segments that connect features to their labels. As a formal investigation of this approach, Bekos et al. [3] introduced *boundary labelling*: all the labels are required to be placed on the boundary of the map and to be connected to their features using leaders. The point where a leader touches the label is called a *port*. Their work initiated a line of research in developing labelling algorithms with different labelling aesthetics, such as minimizing leader crossings, number of bends per leader and sum of leader lengths [1, 2, 4, 5].

In this paper, we study the *1-bend k -sided boundary labelling* problem. The input is an axis-aligned rectangle B and a set of n points (called *sites*) in the interior of B . In addition, the input contains a set of n points on the boundary of B representing the ports on k consecutive sides of B for some $1 \leq k \leq 4$. The objective is to decide whether each site can be connected to a unique

*This work is supported in part by Natural Sciences and Engineering Research Council of Canada (NSERC).

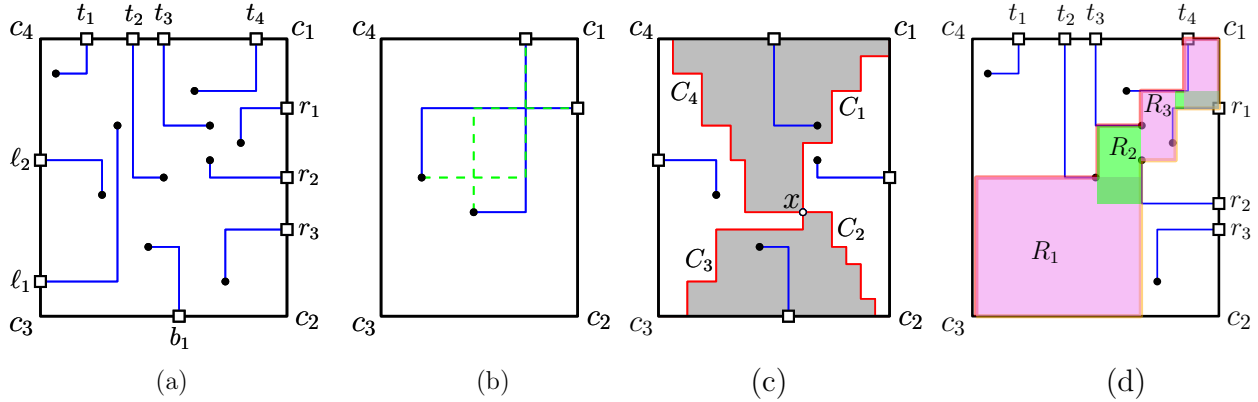


Figure 1: (a) An 1-bend four-sided boundary labelling problem with $w = 4, x = 3, y = 1$ and $z = 2$, (b) an instance of the 1-bend two-sided boundary labelling problem with no planar solution with 1-bend leaders, and (c) a partitioned solution. (d) The sequence of empty rectangles.

port using an axis-aligned leader with at most 1 bend such that the leaders are disjoint and each leader lies entirely in the interior of B , except the endpoint that is attached to a port. Figure 1(a) illustrates a labelling for a 1-bend k -sided boundary labelling instance. If such a solution exists, then we call it a *feasible* solution and say that the problem is *solvable*. Notice that not every instance of the boundary labelling problem is solvable; see Figure 1(b).

Related work. The boundary labelling problem was first formulated by Bekos et al. [3] who solved the 1-bend one-sided and 1-bend two-sided models (when the ports lie on two opposite sides of R) in $O(n \log n)$ time. They also gave an $O(n \log n)$ -time algorithm for the 2-bend four-sided boundary labelling problem (i.e., when each leader can have at most 2 bends).

Kindermann et al. [11] examined k -sided boundary labelling, where the ports appear on adjacent sides. For the 1-bend two-sided boundary labelling problem, they gave an $O(n^2)$ -time algorithm. For 1-bend three- and four-sided models of the problem, they gave $O(n^4)$ - and $O(n^9)$ -time algorithms, respectively. If a boundary labelling instance admits an affirmative solution, then it is desirable to seek for a labelling that optimizes a labelling aesthetic, such as minimizing the sum of the leader lengths or minimizing the number of bends per leader. For minimizing the sum of leader lengths, Bekos et al. [3] gave an exact $O(n^2)$ -time algorithm for the 1-bend one-sided and 1-bend (opposite) two-sided models; their algorithm for 1-bend one-sided model was later improved to an $O(n \log n)$ -time algorithm by Benkert et al. [4].

Kindermann et al. [11] gave an $O(n^8 \log n)$ -time dynamic programming algorithm for the 1-bend (adjacent) two-sided model. Bose et al. [5] (see [6] for the full version) improved this result by giving an $O(n^3 \log n)$ -time dynamic programming algorithm. They also showed that the 1-bend three- and four-sided problems (for the sum of the leader length minimization) can be reduced to the maximum independent set problem on outerstring graphs. The idea is to, for each site, obtain n leaders by connecting the site to every port. Consider each leader as an outerstring (i.e., a polygonal curve that has one endpoint attached to the boundary of an enclosing rectangle). This forms an outerstring graph. Then, by an appropriate weight assignment for edges, the boundary labelling problem is equivalent to the maximum-weight independent set problem on this outerstring graph. Since we have $O(n^2)$ outerstrings (where n is the number of sites) and maximum-weight

independent set can be solved in $O(N^3)$ time on outerstring graphs (here, N is the complexity of geometrically representing the input graph) [10], they obtain an $O(n^6)$ -time algorithm for the three- and four-sided boundary labelling problem. However, it is not obvious whether this approach can be used to obtain a faster algorithm for the decision version, where we do not require leader length minimization.

Other models for boundary labelling such as labelling with sliding ports [4], dynamic boundary labelling [14], boundary labelling with octilinear leaders [2], many-to-one boundary labelling [13, 12] and boundary labelling in the presence of obstacles [8] has also been studied. Moreover, see [4, 5] for results on bend minimization. Throughout the paper, we consider 1-bend leaders, which are also known as *po-leaders* [3].

Our results. In this paper, we give algorithms with running times $O(n^3 \log n)$ and $O(n^5)$ for the 1-bend three-sided and four-sided boundary labelling problems, which improves the previously best known algorithms by nearly a linear factor.

The fastest known algorithm for the three-sided model was Kindermann et al.’s [11] $O(n^4)$ -time algorithm that reduced the problem into $O(n^2)$ two-sided boundary labelling problems. While we also use their partitioning technique, our improvement comes from a dynamic programming approach that carefully decomposes three-sided problems into various simple shapes that are not necessarily rectangular. We prove that such a decomposition can be computed fast using suitable data-structures. The crux of our approach is to show new properties of simpler types of problems and then using them as building blocks to solve the main labelling problem.

For the four-sided model, the fastest known algorithm was the $O(n^6)$ -time algorithm of Bose et al. [5] that reduced the problem into the maximum independent set problem in an outerstring graph. We show that Kindermann et al.’s [11] observation on partitioning two-sided boundary labelling problems using a xy -monotone curve can be used to find a fast solution for the four-sided model. Such an approach was previously taken by Bose et al. [5], but it already took $O(n^3 \log n)$ time for the 2-sided model, and they eventually settled with an $O(n^6)$ -time algorithm for the four-sided model. With the four sides involved, designing a decomposition with a few different types of shapes of low complexity becomes challenging. Our improvement results from a systematic decomposition that generates a small number of subproblems at the expense of using a larger size dynamic programming table, resulting in an $O(n^5)$ -time algorithm.

2 Preliminaries

In this section, we give some notation and preliminaries that will be used in the rest of the paper. For a point p in the plane, we denote the x - and y -coordinates of p by $x(p)$ and $y(p)$, respectively. Consider the input rectangle B and let c_1, \dots, c_4 denote the corners of B that are named in clockwise order such that c_1 is the top-right corner of B . Let $B_{\text{top}}, B_{\text{bottom}}, B_{\text{left}}$ and B_{right} denote the top, bottom, left and right sides of B , respectively. We refer to a port as a *top port* (resp., *bottom*, *left* and *right port*), if it lies on B_{top} (resp., $B_{\text{bottom}}, B_{\text{left}}$ and B_{right}). Similarly, we call a leader a *top leader* (resp., *bottom*, *left* and *right leader*), if it is connected to a top port (resp., bottom, left and right port).

Let w, x, y, z be the number of ports on the top, right, bottom and left side of B ; notice that $w+x+y+z = n$. We denote these ports as $t_1, \dots, t_w, r_1, \dots, r_x, b_1, \dots, b_y$ and ℓ_1, \dots, ℓ_z in clockwise order. See Figure 1(a) for an example. We assume that the sites are in general position; i.e., the

number of sites and ports on every horizontal (similarly, vertical) line that properly intersects B is at most one. For the rest of the paper, whenever we say a rectangle, we mean an axis-aligned rectangle.

For a point x inside B , consider the rectangle B_i that is spanned by x and c_i , where $1 \leq i \leq 4$. Each rectangle B_i contains only two types of ports; e.g., B_1 contains only top and right ports. A feasible solution for a solvable instance of a boundary labelling problem is called *partitioned*, if there exists a point x such that for each rectangle B_i , there exists an axis-aligned xy -monotone polygonal curve C_i from x to c_i that separates the two types of leaders in B_i . That is, every pair of sites in B_i that lie on different sides of C_i are connected to ports that lie on different (but adjacent) sides of B . See Figure 1(c). We refer to the polygonal curve as the *xy-separating curve*. Kindermann et al. [11] observed that if an instance of a boundary labelling problem admits a feasible solution, then it must admit a partitioned solution.

Lemma 2.1 (Kindermann et al. [11]). *If there exists a feasible solution for the 1-bend four-sided boundary labelling problem, then there also exists a partitioned solution for the problem.*

Consider a two-sided problem where the ports are on B_{top} and B_{right} . Assume that the problem has a feasible solution, and let C be an xy -separating curve. Let *above*(C) (resp., *below*(C)) be the polygonal regions above C (resp., below C) that is bounded by B_{top} and B_{left} (resp., by B_{right} and B_{bottom}). Now, let C_u (resp., C_b) be the xy -separating curve that minimizes the area of *above*(C) (resp., *below*(C)). Given C_u and C_b , we construct a sequence of rectangles as follows (see Figure 1(d)).

- Each rectangle is a maximal rectangle between C_u and C_b .
- The bottom-left corner of R_1 is c_3 . Since R_1 is maximal, it is uniquely determined.
- Let $i > 1$. We know that the top and right sides of R_{i-1} are determined by a pair of leaders L^t and L^r , respectively. Let $a \in L^t$ be the rightmost point on the top side of R_{i-1} , and let $b \in L^r$ be the topmost point on the right side of R_{i-1} . Then the rectangle R_i is the maximal empty rectangle whose bottom-left corner is $(x(a), y(b))$ and that is bounded by C_u and C_b .

We say that an instance of the problem is *balanced* if it contains the same number of sites and ports. We next show the following result that will be useful in the following sections.

Lemma 2.2. *Let P be a 1-bend one-sided boundary labelling problem with a constraint that the leftmost and rightmost ports a, c on B_{top} must be connected to a pair of points b, d , respectively. Let s be the rightmost or bottommost site of the problem excluding b and d . If P has a feasible solution satisfying the given constraint, then it also has a solution with connects s to the first port t_j (while walking from c to a along the boundary) that decomposes the problem into two balanced subproblems.*

Proof. First, assume that s is the bottommost point (see Figure 2(a)–(b)). Assume for a contradiction that connecting s to t_j would not give a feasible solution, whereas there is another port t_i such that connecting s to t_i would yield a feasible solution.

Note that t_i lies to the left of t_j . Let L be the leader of t_i . We swap the leaders of t_i and t_j . Such a swap may introduce crossings in the rectangular region R to the right side of L . However, after the swap both sides of the leader of t_j in R are balanced one-sided problems (see Figure 2(c)). Such a solution with crossings to a 1-sided boundary labelling problem can always be made planar

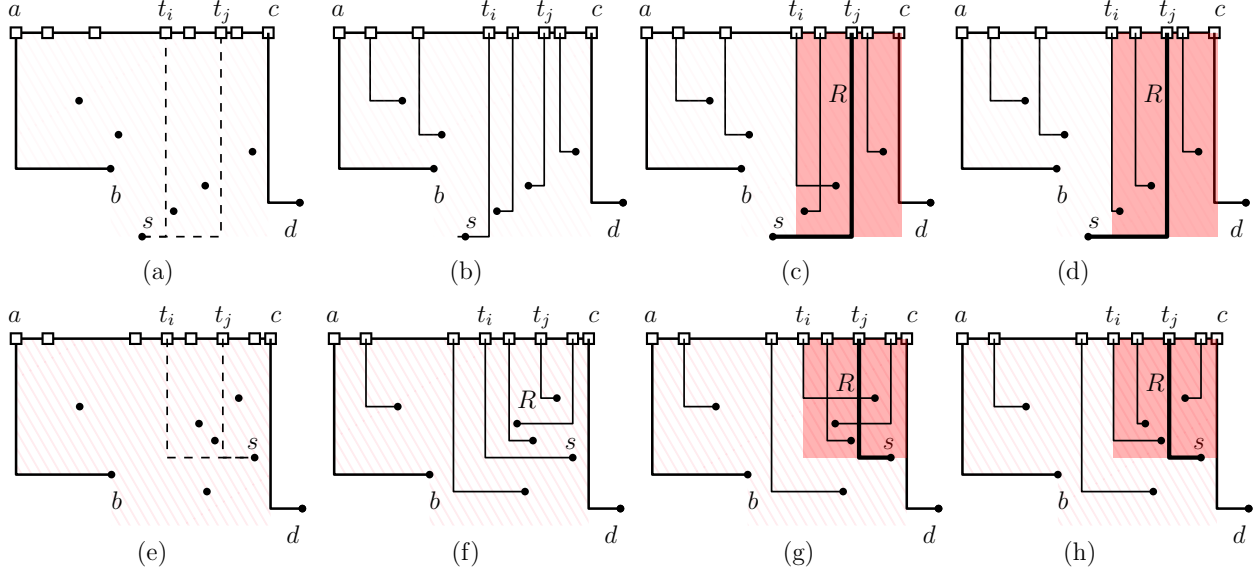


Figure 2: An illustration in supporting the proof of Lemma 2.2.

by local swaps [4]. The proof for the case when s is the rightmost point is the same. Figure 2(e)–(h) illustrate such a scenario. \square

3 Three-Sided Boundary Labelling

In this section, we give an $O(n^3 \log n)$ -time algorithm for the three-sided boundary labelling problem. We assume that the ports are located on B_{left} , B_{top} and B_{right} . Kindermann et al. [11] gave an $O(n^4)$ -time algorithm for this problem as follows. Consider the grid induced by a horizontal and a vertical line through every port and site. For each node of this grid, they partition the three-sided problem into an L -shaped two-sided and a Γ -shaped two-sided problem (Figure 3(a)–(b)). They showed that the three-sided problem is solvable if and only if there exists a grid node whose two two-sided problems both are solvable.

3.1 Algorithm Overview

We also start by considering every grid node x , but we employ a dynamic programming approach that expresses the resulting two-sided subproblems by x and a port. We show that the two-sided subproblems can have $O(1)$ different types. This gives us $O(1)$ different tables, each of size $O(n^3)$. We show that the running time to fill all the entries is $O(n^3 \log n)$. For a grid node x , let x' be the projection of x onto B_{top} . The point x' splits the ports on B into two sets: those to the left of x' and those to the right of it. This means that the line segment xx' can be extended to an axis-aligned curve with two bends that splits the problem into two balanced L - and Γ -shaped two-sided subproblems; see Figure 3. Kindermann et al. [11] observed that such a balanced partition is unique. Hence if there exists a balanced partition by extending xx' to a 2-bend curve, then there must be a unique position where the number of sites to the left of the curve matches the number of ports to the left of x' .

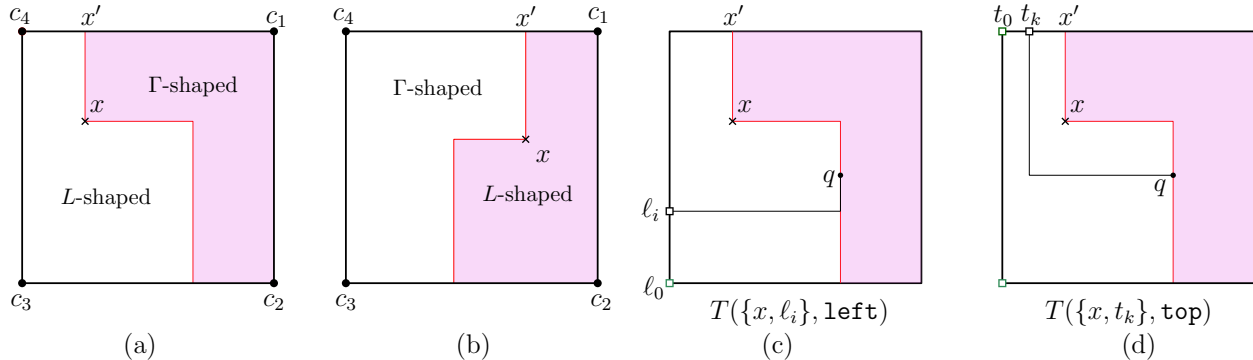


Figure 3: (a)–(b) An L - and a Γ -shaped problem. (c)–(d) Encoding of the L -shaped problems. The site q that determines the boundary of the L -shape can be recovered from the encoding.

In the following, we describe the details of solving the L - and Γ -shaped two-sided problems. W.l.o.g., we assume that the two-sided problem contains the top-left corner c_4 of B . While decomposing an L -shaped problem, we will reduce it either into a smaller L -shaped problem or a rectangular two-sided problem. Decomposition of Γ -shaped problem is more involved.

3.2 Solving an L -Shaped Problem

We denote an L -shaped subproblem with a grid node x and a port b , where b lies either on B_{top} or B_{left} . If b is a port on B_{left} (i.e., $b = \ell_i$ for some i), then we denote the subproblem by $T(\{x, \ell_i\}, \text{left})$ in which the bottom side is determined by a horizontal line through ℓ_i (e.g., see Figure 3(c)). Here, the last parameter denotes whether the port belongs to B_{left} or B_{top} . Initially, we assume a dummy port ℓ_0 located at c_3 and so our goal is to compute $T(\{x, \ell_0\}, \text{left})$. On the other hand, if $b = t_k$ for some k (i.e., it is a port on B_{top}), then we define the problem as $T(\{x, t_k\}, \text{top})$ (see Figure 3(d)). Here, the goal is to compute $T(\{x, t_0\}, \text{top})$, where t_0 is a dummy port at c_4 .

To decompose $T(\{x, \ell_i\}, \text{left})$, we find the rightmost site p of the subproblem in $O(\log n)$ time (Figure 4(a)). We first do some preprocessing, and then consider two cases depending on whether p lies to the left or right side of the vertical line through x .

For the preprocessing, we keep the sites and ports in a range counting data structure that supports $O(\log n)$ counting query [7]. Second, for each horizontal slab determined by a pair of horizontal grid lines h, h' (passing through sites and ports), we keep the points inside the slab in a sorted array $M(h, h')$, which takes $O(n^3 \log n)$ time. We now use these data structures to find p . We first compute the sites and ports in the rectangle determined by the diagonal c_4x , and then find the number of points needed in $O(\log n)$ time. Finally, we find a site r (that balances the number of sites and points) in $O(\log n)$ time by a binary search in the array M for the slab determined by the horizontal grid lines through ℓ_i and x . If r lies to the right of the vertical line through x , then r is the desired point p . Otherwise, p lies to the left of the vertical line through x , and we can find p by searching in the array M for the slab determined by the horizontal grid lines through ℓ_i and t_0 . We will frequently search for such a unique site throughout the paper and so we will use a similar preprocessing.

Case 1 (p lies to the right side of the vertical line through x). We connect p to the “right” port: after connecting, the resulting subproblems are balanced; i.e., the number of sites in each resulting subproblem is the same as the number of ports of that subproblem. There might be several ports that are right in this sense, but one can apply Lemma 2.2 (assuming dummy leaders as boundary constraints) to show that the subproblem has a feasible solution if and only if there exists a feasible solution connecting p either to the bottommost or to the rightmost port that satisfies the balanced condition. Once we find p and the appropriate port c for p , there are three possible scenarios as illustrated in Figure 4. We can decompose the subproblem using the following recursive formula (depending on whether p is connected to B_{left} or B_{top}):

$$T(\{x, \ell_i\}, \text{left}) = \begin{cases} T(\{x, \ell_j\}, \text{left}) \wedge T' & \text{e.g., see Figure 4(a)–4(b), or} \\ T(\{x, t_j\}, \text{top}) \wedge T(\{y, \ell_i\}, \text{left}) & \text{e.g., see Figure 4(c)} \end{cases}$$

Here, $T(\{x, t_j\}, \text{top})$ is an L -shaped one-sided problem and T' is a rectangular one-sided problem. There always exists a solution for the balanced rectangular one-sided problem [4], and thus T' can be considered as true. Since $T(\{x, t_j\}, \text{top})$ is balanced, we can show that there always exists a solution for $T(\{x, t_j\}, \text{top})$, as follows. First assume that the vertical line through x does not pass through a port (see Figure 5(a)). Let t be the rightmost port in $T(\{x, t_j\}, \text{top})$, and let Q be the set of points inside the rectangle R_x determined by diagonal xq . Scale down the rectangle R_x horizontally and translate the rectangle inside the vertical slab determined by the vertical lines through t and x . There always exists a solution for the balanced rectangular one-sided problem [4], we can translate the points back to their original position extending the leaders as necessary. The case when the vertical line through x passes through a port t_x can be processed in the same way, by first connecting t_x to the topmost point of R_x , and then choosing the port immediately to the left of t_x as t . We thus have the following recurrence formula.

$$T(\{x, \ell_i\}, \text{left}) = \begin{cases} T(\{x, \ell_j\}, \text{left}) & \text{if } \ell_j \text{ exists, e.g., see Figure 4(a)–4(b), or} \\ T(\{y, \ell_i\}, \text{left}) & \text{if } t_j \text{ exists, e.g., see Figure 4(c)} \end{cases}$$

We now show how to find the point p and then decompose $T(\{x, \ell_i\}, \text{left})$. The table $T(\{x, \ell_i\}, \text{left})$ is of size $O(n^3)$. We will show that each subproblem can be solved by a constant number of table look-ups, and these entries can be found in $O(\log n)$ time. Hence, the overall computation takes $O(n^3 \log n)$ time.

We now show how to find the “right” port c for p . First, assume that c is a port ℓ_j on B_{left} (see Figure 4(a)–(b)). We need another $O(n^3 \log n)$ -time preprocessing as follows. Define a table $M'(s, \ell_i)$, where s is a site, and ℓ_i is a port on B_{left} . At the entry $M'(s, \ell_i)$, we store the port ℓ_j such that $j > i$ is the smallest index for which the rectangle defined by B_{left} , the horizontal lines through ℓ_i, ℓ_j and the vertical line through s contains exactly $(j - i - 1)$ sites. We set j to 0 when no such port ℓ_j exists. The table M' has size $O(n^2)$ and we can fill each entry of the table in $O(n \log n)$ time; hence, we can fill out the entire M' in $O(n^3 \log n)$ time. Observe that the port c for p is stored in $M'(p, \ell_i)$.

Consider now the case when c is a port t_j on B_{top} (see Figure 4(c)). We again rely on an $O(n^3 \log n)$ -time preprocessing. For every site s and a vertical grid line ℓ (passing through a port or a site) to the left of s , we keep a sorted array $M''(s, \ell)$ of size $O(n)$. Each element of the array corresponds to a rectangle bounded by the horizontal line through s , B_{top}, ℓ , and another vertical grid line ℓ' through a port to the left of ℓ . The rectangles are sorted based on the difference between

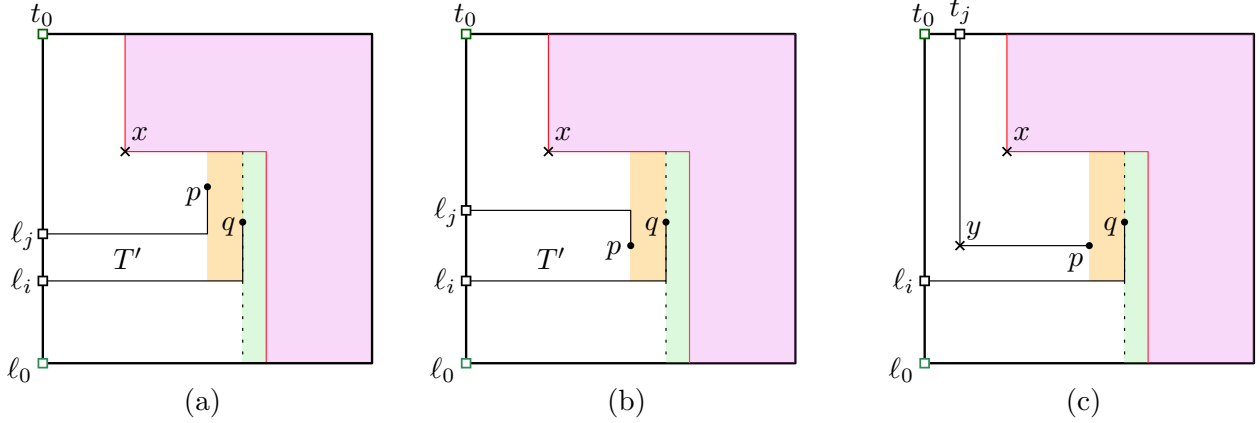


Figure 4: The decomposition of an L -shaped problem when $b = \ell_i$.

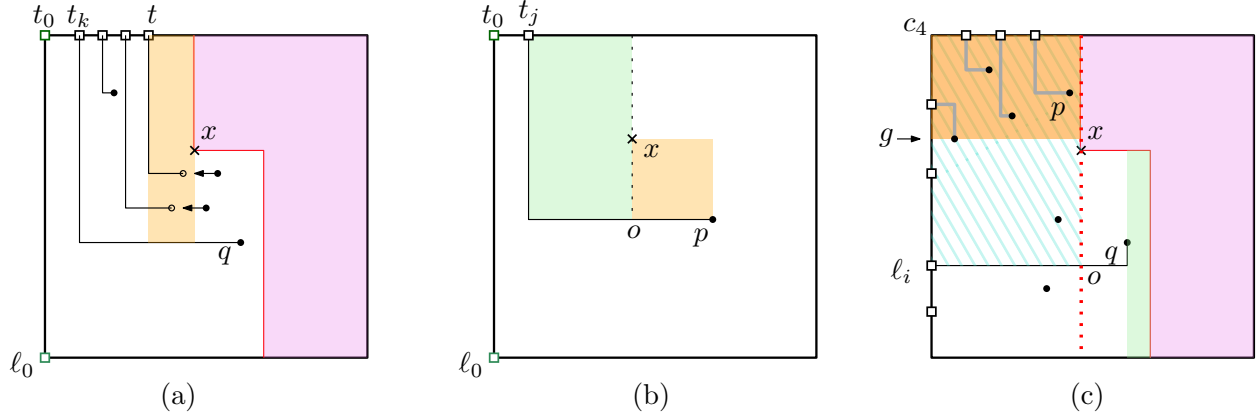


Figure 5: (a) Reducing $T(\{x, t_j\}, \text{top})$ to a rectangular one-sided problem, and (b) finding the port c for p when $c = t_j$ for some j . (c) Precomputation of the two-sided problems.

the sites and ports and then by the x -coordinate of ℓ' . Consequently, to find $c(=t_j)$, we can look for the number of sites in the rectangle determined by the diagonal px (see Figure 5(b)), and then binary search for that number in the precomputed array for $M''(p, x)$.

Case 2 (p lies to the left side of the vertical line through x). Let o be the intersection of the vertical line through x and the leader connecting ℓ_i and q (see Figure 5(c)). Since p is the rightmost point, it suffices to solve the rectangular two-sided problem P determined by the rectangle with diagonal oc_4 (shown in falling pattern). We will determine whether a solution exists in $O(1)$ time based on some precomputed information, as follows.

For each vertical grid line, we will precompute the topmost horizontal grid line g such that the two-sided problem (shown in orange) determined by these lines, B_{top} and B_{left} has a feasible solution. If g lies above ℓ_i , then the two-sided problem is solvable (as the remaining region determines a balanced one-sided problem); otherwise, it is not solvable. We will use the known $O(n^2)$ -time algorithm [11] to check the feasibility of a two-sided problem, which looks for a “partitioned” solution. However, we do not necessarily require our two-sided problem to be partitioned.

We now show that the precomputation takes $O(n^3 \log n)$ time. For every vertical grid line v , we first compute a sorted array A_v of horizontal grid lines such that the two-sided problem determined by v and each element of A_v is balanced. This takes $O(n \log n)$ time for v and $O(n^2 \log n)$ time for all vertical grid lines. For each v , we then do a binary search on A_v to find the topmost grid line g such that the corresponding two-sided problem has a feasible solution. Since computing a solution to the two-sided problem takes $O(n^2)$ time [11], g can be found in $O(n^2 \log n)$ time for v , and in $O(n^3 \log n)$ time for all the vertical grid lines.

Remark. While decomposing L -shapes, we always find the rightmost point p . If the x -coordinate of p is larger than that of x , then the subproblems $T(\{x, \ell_j\}, \mathbf{left})$ and $T(\{y, \ell_i\}, \mathbf{left})$ are also L -shaped. Otherwise, the problem reduces to a rectangular one-sided or two-sided problem. Hence a Γ -shape problem does not appear during the decomposition of L -shaped problems.

3.3 Solving a Γ -Shaped Problem

Consider the Γ -shaped problem containing the top-left corner c_4 ; see e.g. Figure 6(a). Let o be the projection of x onto B_{bottom} , and let y be the other bend of the Γ shape. In the following, we refer to the rectangle with diagonal oy as the *forbidden region*.

Kindermann et al. [11, Lemma 8] observed that there must exist an axis-aligned xy -monotone curve C that connects c_4 to x such that the sites above C are connected to top ports and the sites below C are connected to left ports. We extend C to o along the vertical line xo (e.g., see Figure 6(b)). Since no leader will enter the forbidden region, we can now consider C as a separating curve for a two-sided problem determined by the rectangle with diagonal c_4o . For any partitioned solution, we can compute a sequence of maximal empty rectangles, as we discussed in Section 2, such that the lower-right corner of R_1 coincides with o . To decompose the problem, consider the first rectangle R_1 in this sequence. The rectangle R_1 can either cover the forbidden region entirely or partially in three different ways; see Figure 6(b). Since the separating curve through the grid point x (Figure 6(a)) determines a partition, the leaders of the Γ -shape must not enter into the forbidden region. Therefore, it suffices to consider an empty rectangle R_1 that entirely covers the forbidden region.

Since R_1 is maximal, the top or left side of R_1 must contain a site (e.g., see Figure 6(c)); because otherwise, the leaders that determines the top and left side of R_1 will cross. Assume w.l.o.g. that the top side of R_1 contains a site p that is connected to a port $b(= t_k)$. Notice that b cannot be a left port because it contradicts the existence of the curve C . Moreover, the left side of R_1 either contains a site or it is aligned with a leader that connects a port ℓ_j to a site q . The bottom row in Figure 6 shows all possible scenarios; notice that q cannot be connected to a top port, again because of having C . This decomposes the problem into three subproblems (see Figure 6(d)). Two one-sided subproblems Q_1 and Q_2 , and a smaller two-sided subproblem. Q_1 is bounded by the leader connecting ℓ_j to q , the left side of R_1 , B_{bottom} and B_{left} . The subproblem Q_2 is bounded by the leader connecting p to t_k , B_{top} , the curve determined by x , and the top side of R_1 .

The smaller two-sided subproblem is bounded by $B_{\text{left}}, B_{\text{top}}$, the leaders incident to t_k and ℓ_j , and the boundary of R_1 . We solve such two-sided problems by finding a sequence of maximal empty rectangles as described in Section 2. The idea is inspired by Bose et al.'s [5] approach to solve a two-sided problem using a compact encoding for the table. Since we do not optimize the sum of leader lengths, our approach is much simpler.

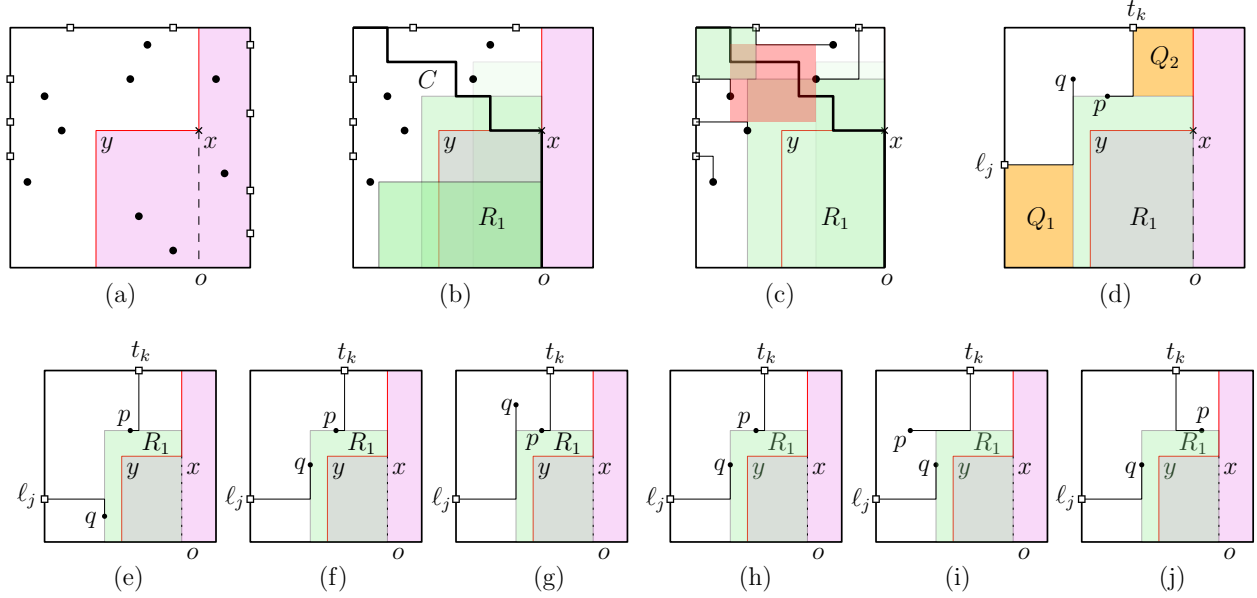


Figure 6: (a) A Γ -shaped problem. (b)–(c) Three possibilities for the empty rectangle R_1 , and a sequence of maximal rectangles corresponding to the separating curve. (d) Rectangle R_1 decomposes the problem into two one-sided subproblems and a smaller two-sided subproblem. (e)–(j) All possible cases for the two leaders determining the top and left sides of R_1 .

Decomposing two-sided subproblems. To decompose the two-sided subproblems, we use the following observation.

Lemma 3.1 (Bose et al. [5]). *If a two-sided boundary labelling problem with sites on B_{top} and B_{left} has a feasible solution, then there exists a partitioned solution where every maximal empty rectangle contains a site either on its top or on its left side.*

We first describe how to represent the two-sided problems. If the maximal empty rectangle R contains a site on its top side (Figure 6(g)), then we represent the problem with the ports and the x -coordinate of the left side of R , i.e., t_k, ℓ_j and x -coordinate of q . Otherwise, we use the ports and the y -coordinate of the top side of R .

Formally, define a table $T_y(\ell_i, t_j, z)$ (resp., $T_x(\ell_i, t_j, z)$), where ℓ_i and t_j are two ports and z denotes the y -coordinate (resp., x -coordinate) of the site to which the port t_j (resp., ℓ_i) is connected (see Figure 7). Given $T_x(\ell_i, t_j, z)$ (similarly, $T_y(\ell_i, t_j, z)$), we can completely determine the problem boundary, as follows. Note that by definition the left side of R (the rectangle that defined the subproblem, shown in pink) has the x -coordinate z . Hence the site of t_j lies on the top side of R (by Lemma 3.1). We can thus perform a binary search to find this site. Once we have the two sites (and so the two incident leaders), we can find the lower right corner q for the next candidate rectangle as defined in Section 2.

We now show how to compute $T_x(\ell_i, t_j, z)$; the other is symmetric. After we determine the lower right corner q for the next subsequent rectangle, we look for all candidate maximal empty rectangles R' with lower right corner q . Consider now one such candidate rectangle R' (shown in orange in Figure 7), and let $\ell_{i'}$ and $t_{j'}$ be the ports defining its left and top sides, respectively. This now decomposes $T_x(\ell_i, t_j, z)$ into three subproblems; namely, two one-sided subproblems defined

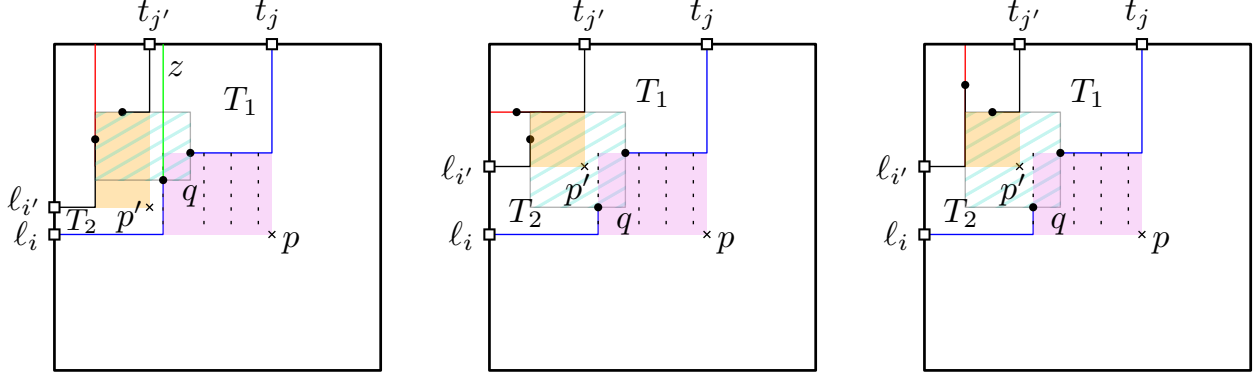


Figure 7: An illustration for solving the two-sided subproblems arising in a Γ -shaped problem.

by $\ell_i, \ell_{i'}$ and $t_j, t_{j'}$, and a two-sided subproblem. By Lemma 3.1, R' contains a site on its top or left side. If the top side of R' contains a site, then we look-up the entry $T_x(\ell_{i'}, t_{j'}, z)$; otherwise, we look-up the entry $T_y(\ell_{i'}, t_{j'}, z)$. We hence have the following recurrence relation.

$$T_x(\ell_i, t_j, z) = \begin{cases} T_x(\ell_{i'}, t_{j'}, z) \wedge T_1 \wedge T_2 & \text{if the top side of } R' \text{ contains a site,} \\ & \text{e.g., see Figure 7(left) and Figure 7(right)} \\ T_y(\ell_{i'}, t_{j'}, z) \wedge T_1 \wedge T_2 & \text{if the top side of } R' \text{ does not contain a site,} \\ & \text{e.g., see Figure 7(middle).} \end{cases}$$

Here, T_1 and T_2 are one-sided problems, bounded by two leaders and a maximum empty rectangle. In the following, we discuss how to solve these problems.

Solving one-sided problems. If T_i , where $i \in \{1, 2\}$, is a balanced rectangular one-sided problem (Figure 8(d)–(e)), then it has a feasible solution [4]. If T_i is L -shaped and bounded by one side of the maximum empty rectangle (Figure 8(f)), then it can be reduced to a rectangular one-sided problem, as described in Section 3.2. Otherwise, the boundary of T_i contains two sides of the maximal empty rectangle (Figure 8(a)–(b)), or one side of the maximal empty rectangle and two vertical segments of the two leaders (Figure 8(c)). In such a case, we can decide whether it has a feasible solution in $O(\log n)$ time, as follows.

Let o, o' be the bottom-left corner of the empty rectangle R' and the bend point of the leader of ℓ_i (Figure 8(a)–(c)), respectively. Let c be the number of sites in the open rectangle determined by the diagonal oo' . Let ℓ be a port such that there are c ports between ℓ_i and ℓ (including ℓ). If the y -coordinate of ℓ is not larger than that of o (or a , if a is below o), then we can decompose the problem into two subproblems such that both of them have a feasible solution. One of these subproblems is a rectangular one-sided problem (shown in pink), and the other is an L -shaped one-sided problem (shown in green). Both of them are balanced. The existence of a solution is immediate from [4] for the rectangular case. The existence of a solution for the L -shaped case is by the reduction to a one-sided rectangular problem (Section 3.2). If the y -coordinate of ℓ is larger than that of o (or that of a , if a is below o), then there does not exist a solution with leaders not intersecting the empty rectangle R' (or the leader of ℓ_i).

Note that the table T_x and T_y are of size $O(n^3)$ and each subproblem can be solved by examining a set of candidate rectangles. Bose et al. [5] observed that the number of such candidate rectangles

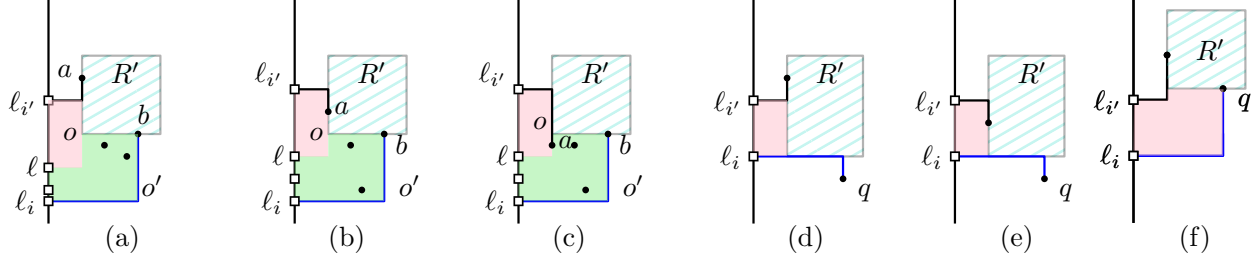


Figure 8: An illustration for solving the one-sided subproblems arising in a Γ -shaped problem.

is $O(n^3)$, and while searching for candidate rectangles, no rectangle appears more than once. Thus the total number of table look ups is bounded by $O(n^3)$. Furthermore, all these rectangles can be precomputed in $O(n^3 \log n)$ time [5]. Hence, the overall time to solve a Γ -shaped problem is $O(n^3 \log n)$. The following theorem summarizes the result of this section.

Theorem 3.1. *Given a 1-bend three-sided boundary labelling problem with n sites and n ports, one can find a feasible solution (if exists) in $O(n^3 \log n)$ time.*

4 Four-Sided Boundary Labelling

In this section, we give an $O(n^5)$ -time dynamic programming algorithm for the four-sided boundary labelling.

4.1 Algorithm Overview

Our dynamic programming solution will search for a set of maximal empty rectangles R_1, \dots, R_k corresponding to the xy -separating curve, as described in Section 2. The intuition is to represent a problem using at most two given leaders. For example, in Figure 9(a) the first empty rectangle is R_1 , with the top and right sides of R_1 determined by the leaders of ℓ_2 and b_2 , respectively. The problem will have a feasible solution with these given leaders if and only if the subproblems P_1 and P_2 (shown in falling and rising patterns, respectively) have feasible solutions. Since the subproblems must be balanced, given the two leaders adjacent to P_2 (see Figure 9(a)), we can determine the boundary of the problem. We will use this idea to encode the subproblems.

It may initially appear that to precisely describe a subproblem, one should need some additional information along with the two given leaders. For example, the dashed boundary in Figure 9(b). However, such information can be derived from the given leaders. Here, the top-right corner of R_1 (hence, the dashed line) can be recovered using the y -coordinate of the bottommost point of the leader of ℓ_2 , and the x -coordinate of the leftmost point of the leader of b_2 . We will try all possible choices for the first empty rectangle R_1 . In a general step, we will continue searching for the subsequent empty rectangle. For example, consider the subproblem in Figure 9(b). For a subsequent empty rectangle, we will decompose the problem into at most three new subproblems (Figure 9(c)). Each of these new subproblems can be represented using at most two leaders.

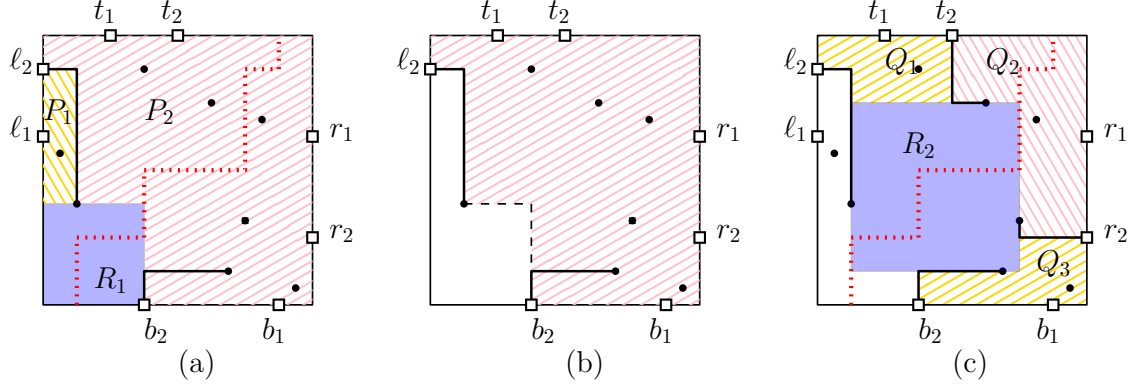


Figure 9: The idea of decomposing a problem into subproblems.

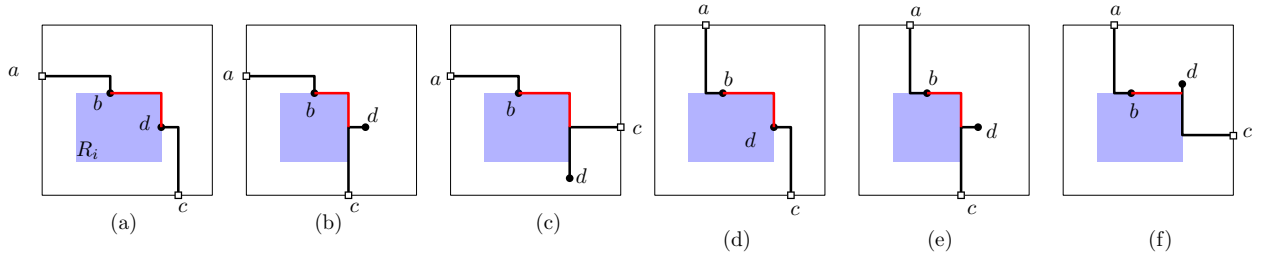


Figure 10: Recovering the boundary (red) from the leaders when R_i contains a site on its top side.

4.2 Solving Subproblems

We will distinguish the subproblems depending on whether they contain the top-right corner c_1 of the rectangle B or not. We first outline the case when a subproblem contains c_1 .

A subproblem contains c_1 . We denote a subproblem that contains c_1 by $T(a, b, c, d)$. Here, a, c are the two ports on the opposite sides of the separating curve, and b and d are their corresponding sites. Given a, b, c, d , we can completely determine the boundary of the subproblem, as follows. Let p and q be a pair of points on the leaders of a and c , respectively, with the minimum Euclidean distance. Then, the rectangle with diagonal pq determines the boundary of the subproblem. Figure 10 illustrates the cases (up to the horizontal or vertical reflection of the sites), where the maximal empty rectangle R_i contains a site on its top side. The recovered boundary is shown in red. On the other hand, Figure 11 illustrates the cases when R_i does not contain any site on its top or right side. If there are several choices for p, q , then we take the one with the smallest y -coordinate (or, symmetrically smallest x -coordinate) as illustrated in Figure 11(d).

We now show how to decompose subproblems containing c_1 . Since we are searching for a partitioned solution, the decomposition must contain at least one such subproblem. Let R_i be the empty rectangle associated with $T(a, b, c, d)$ (Figure 12(a)). First assume the case when c is on B_{left} and a is on B_{bottom} . Let p, q be the pair of points with the minimum Euclidean distance between the leaders of c and a . Let R_{pq} be the rectangle with diagonal pq . Note that we can choose the bottom left corner of R_{pq} as the bottom left corner of the subsequent empty rectangle R_{i+1} . There are $O(n^2)$ choices for the top-right corner of R_{i+1} . Thus trying all these subproblems would

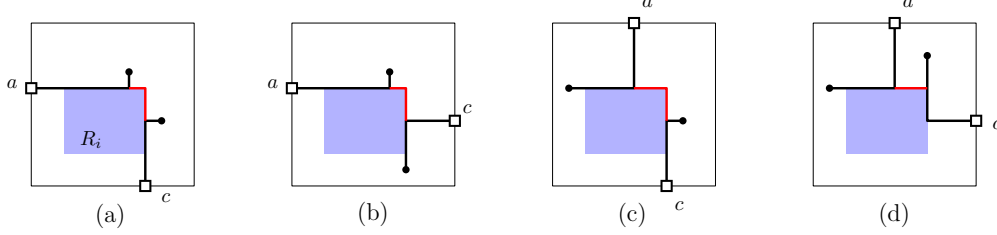


Figure 11: Recovering the boundary (red) when R_i does not contain sites on its top or right side.

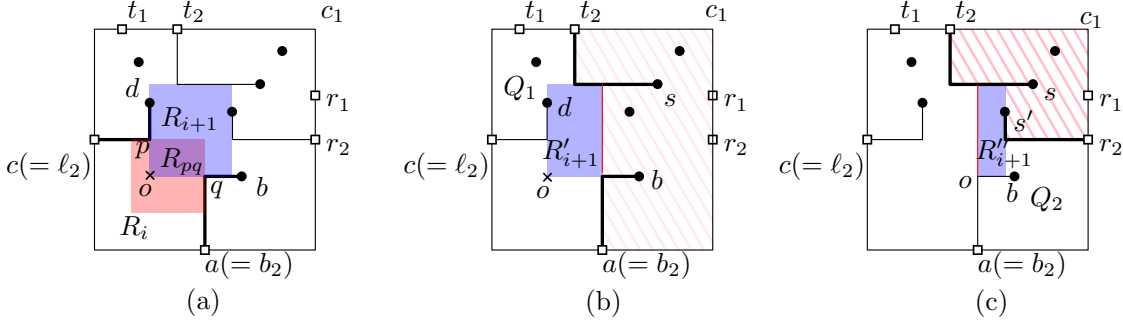


Figure 12: Decomposition of a subproblem.

take $O(n^2)$ time to fill the table entry corresponding to $T(a, b, c, d)$.

Instead of searching for R_{i+1} directly, we first extend R_{pq} vertically (Figure 12(b)) and then horizontally (Figure 12(c)). Thus the subsequent rectangle R'_{i+1} in our approach will have $O(n)$ choices for the top boundary. The leader L that determines the top boundary will partition the problem into two subproblems: one is a problem that includes c_1 , and the other problem Q_1 is either a one-sided or a two-sided subproblem depending on the position of L . For example, in Figure 12(b), $T(a, b, c, d) = T(a, b, t_2, s) \wedge Q_1$.

Note that sometimes R_{pq} can be extended only in one direction. For example, in Figure 12(c), we have $T(a, b, t_2, s)$, and R_{pq} is a vertical line bounded by the leaders, as shown in red. In this case we extend R_{pq} horizontally and we have $O(n)$ choices for its right boundary. The leader L' that determines the right boundary (i.e, the one connecting r_2 to s') will partition the problem into two subproblems: one is a problem that includes c_1 , and the other problem Q_2 is either a one-sided or a two-sided subproblem depending on the position of L' . For example, in Figure 12(c), $T(a, b, t_2, s) = T(r_2, s', t_2, s) \wedge Q_2$.

A subproblem excludes c_1 . We first show that these problems must be either one-sided or two-sided. Let Q be the subproblem that includes c_1 . Let Q_1 be a subproblem that excludes c_1 and lies above the separating curve. Then the only available sides of B for Q_1 are B_{left} and B_{top} . Symmetrically, only B_{right} and B_{bottom} are available for Q_2 . If Q_i (where $i \in \{1, 2\}$) is a one-sided problem, then we can process the problem in the same ways as described in Section 3.

Consider now the case of two-sided problems, and assume w.l.o.g. that Q_1 is a two-sided problem. Note that Q_1 contains the top-left corner of B . Since we are searching for a partitioned solution (recall Lemma 2.1), there must be a $(-x, -y)$ -monotone axis-aligned separating curve connecting the bottom-right and the top-left corners of B . Hence, there must exist a sequence of

empty rectangles associated with it. Therefore, we can continue decomposing the problem in the same way as we did for the problems that include c_1 .

4.3 Time Complexity

We maintain the points and ports in an orthogonal range counting data structure (with $O(n \log n)$ -time preprocessing) such that given an axis-aligned rectangle, one can report the number of ports and points interior to the rectangle in $O(\log n)$ time [7].

The encoding of the form $T(a, b, c, d)$ allows us to use a dynamic programming table of size $O(n^4)$. Computing each entry requires examining $O(n)$ candidates for an empty rectangle. Each candidate rectangle divides the problem into at most two new subproblems. If the new subproblems are not balanced, then the candidate rectangle would not give a feasible solution. Otherwise, the new subproblems are balanced. For the two-sided problems we perform table look-up, while the feasibility of the one-sided problems can be decided in $O(\log n)$ time. Once we complete the dynamic programming, we get a set of ports mapped to sites and a set of one-sided problems that are feasible, for which the solution needs to be constructed. Since there can be $O(n)$ such one-sided problems, and each can be solved in $O(n \log n)$ time (either by the algorithm of [4], or by a reduction to the rectangular one-sided case), the total time required is $O(n^2 \log n)$.

We can use the range counting data structure to check whether a subproblem is balanced in $O(\log n)$ time [7]. We can precompute the candidate rectangles for every grid point in $O(n^4 \log n)$ time. Since each table look-up takes $O(1)$ time, filling an entry of the dynamic programming table would take $O(n)$ time for all the $O(n)$ candidate rectangles corresponding to that entry. Hence, the overall running time of the algorithm is $O(n^5)$. The following theorem summarizes the main result of this section.

Theorem 4.1. *Given a 1-bend four-sided boundary labelling problem with n sites and n ports, one can find a feasible labelling (if exists) in $O(n^5)$ time.*

5 Conclusion

In this paper, we gave algorithms with running times $O(n^3 \log n)$ and $O(n^5)$ for the 1-bend three- and four-sided boundary labelling problems, improving the previous algorithms of Kindermann et al. [11] and Bose et al. [5]. The main direction for future work is to improve the running time of our algorithms. Another direction is to study the fine-grained complexity of the problem; e.g., can we find a non-trivial lower bound on the running time? Even a quadratic lower bound is not known. Note that Bose et al.’s algorithm [5] minimizes the sum of leader lengths, but ours do not. It would also be interesting to seek faster algorithms that minimize the sum of leader lengths.

References

- [1] Michael A. Bekos, Sabine Cornelsen, Martin Fink, Seok-Hee Hong, Michael Kaufmann, Martin Nöllenburg, Ignaz Rutter, and Antonios Symvonis. Many-to-one boundary labeling with backbones. *J. Graph Algorithms Appl.*, 19(3):779–816, 2015. [1](#)
- [2] Michael A. Bekos, Michael Kaufmann, Martin Nöllenburg, and Antonios Symvonis. Boundary labeling with octilinear leaders. *Algorithmica*, 57(3):436–461, 2010. [1](#), [3](#)

- [3] Michael A. Bekos, Michael Kaufmann, Antonios Symvonis, and Alexander Wolff. Boundary labeling: Models and efficient algorithms for rectangular maps. *Comput. Geom.*, 36(3):215–236, 2007. [1](#), [2](#), [3](#)
- [4] Marc Benkert, Herman J. Haverkort, Moritz Kroll, and Martin Nöllenburg. Algorithms for multi-criteria boundary labeling. *J. Graph Algorithms Appl.*, 13(3):289–317, 2009. [1](#), [2](#), [3](#), [5](#), [7](#), [11](#), [15](#)
- [5] Prosenjit Bose, Paz Carmi, J. Mark Keil, Saeed Mehrabi, and Debajyoti Mondal. Boundary labeling for rectangular diagrams. In *16th Scandinavian Symposium and Workshops on Algorithm Theory (SWAT 2018), June 18-20, 2018, Malmö, Sweden*, pages 12:1–12:14, 2018. [1](#), [2](#), [3](#), [9](#), [10](#), [11](#), [12](#), [15](#)
- [6] Prosenjit Bose, Paz Carmi, J. Mark Keil, Saeed Mehrabi, and Debajyoti Mondal. Boundary labeling for rectangular diagrams. *CoRR*, abs/1803.10812, 2018. [2](#)
- [7] Mark de Berg, Otfried Cheong, Marc van Kreveld, and Mark Overmars. *Computational Geometry: Algorithms and Applications*. Springer, Berlin Heidelberg, 2008. [6](#), [15](#)
- [8] Martin Fink and Subhash Suri. Boundary labeling with obstacles. In *Proceedings of the 28th Canadian Conference on Computational Geometry (CCCG)*, pages 86–92, 2016. [3](#)
- [9] Herbert Freeman and Sean Marrinan and Hitesh Chitalia. Automated labeling of soil survey maps. In *ASPRS-ACSM Annual Convention, Baltimore, volume 1*, pages 51–59, 1996. [1](#)
- [10] J. Mark Keil, Joseph S. B. Mitchell, Dinabandhu Pradhan, and Martin Vatshelle. An algorithm for the maximum weight independent set problem on outerstring graphs. *Comput. Geom.*, 60:19–25, 2017. [3](#)
- [11] Philipp Kindermann, Benjamin Niedermann, Ignaz Rutter, Marcus Schaefer, André Schulz, and Alexander Wolff. Multi-sided boundary labeling. *Algorithmica*, 76(1):225–258, 2016. [2](#), [3](#), [4](#), [5](#), [8](#), [9](#), [15](#)
- [12] Chun-Cheng Lin. Crossing-free many-to-one boundary labeling with hyperleaders. In *IEEE Pacific Visualization Symposium PacificVis 2010, Taipei, Taiwan, March 2-5, 2010*, pages 185–192, 2010. [3](#)
- [13] Chun-Cheng Lin, Hao-Jen Kao, and Hsu-Chun Yen. Many-to-one boundary labeling. *J. Graph Algorithms Appl.*, 12(3):319–356, 2008. [3](#)
- [14] Martin Nöllenburg, Valentin Polishchuk, and Mikko Sysikaski. Dynamic one-sided boundary labeling. In *18th ACM SIGSPATIAL International Symposium on Advances in Geographic Information Systems (GIS)*, pages 310–319, 2010. [3](#)
- [15] Steven Zoraster. Practical results using simulated annealing for point feature label placement. *Cartography and GIS*, 24(4):228–238, 1997. [1](#)